Removal of arsenic and metal ions from acidic effluents *via* the Fenton reaction method

Y. Wang[1]

Affiliation:
1Beijing Research Institute of Chemical Engineering and Metallurgy, CNNC, Beijing, China.

Correspondence to:
Y. Wang

Email:
jakese@163.com

Synopsis
Arsenic-bearing acidic effluent from hydrometallurgical processes contains many harmful metal ions and must be appropriately treated before discharge. In the present study, arsenic, copper, zinc, aluminum, and magnesium were co-precipitated by means of the Fenton reaction. The precipitates obtained under different conditions were investigated to determine their stability. The results indicate that pH value and hydrogen peroxide (H_2O_2) dosage have significant effects on the removal of various elements. Arsenic, copper, zinc, and aluminum (but not magnesium) can be removed at pH 5–6 and an H_2O_2/As mole ratio of 2 at ambient temperature. The precipitates were mainly amorphous and granular with particle size in the micrometre range. The arsenic concentration in leachate from the toxicity characteristic leaching test was 3.6 mg/L, which proves that the precipitates are effective in fixing arsenic.

Keywords
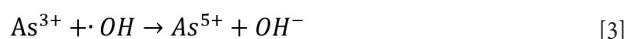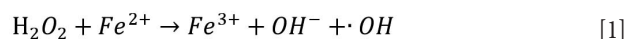acidic effluent, arsenic, coprecipitation, Fenton reaction, metal ions.

Introduction

Arsenic is an extremely toxic substance, which can cause serious harm to humans and animals (Davis *et al.*, 2017; Singh *et al.*, 2015; Mihajlovic *et al.*, 2011). It is generally found in effluents from mining and processing of arsenic-bearing minerals. Therefore, it is necessary to properly treat wastewater before discharge in order to mitigate the environmental impact (Mandal and Suzuki, 2002; Türk *et al.*, 2020).

Co-precipitation of arsenic using ferric salt is one of the common methods in wastewater treatment (Ahmad *et al.* 2020; Ahoranta *et al.*, 2016; Otgon *et al.*, 2019). The arsenic can be removed by precipitation as ferric arsenate or adsorption on the surface of iron oxyhydroxides (Hering *et al.*, 1996; Jain, Raven, and Loeppert, 1999; Qiao *et al.*, 2012). The removal efficiency is strongly related to pH, reaction time, temperature, and dosage of ferric salt (Wickramasinghe *et al.*, 2004; Tang, Wang, and Gao, 2010). The precipitates obtained under ambient conditions are always in the form of ferric arsenate in an amorphous state, which has poor stability and is not suitable for for long-term storage since it can release arsenic into the aqueous environment (Zhu *et al.*, 2006; Berre, Gauvin, and Demopoulos, 2007; Jia *et al.*, 2007). The removal efficiency, as well as the stability of the precipitate, can be increased by adding more ferric salt to adjust the molar ratio of Fe/As to >3 (Chen *et al.*, 2009; Essilfie-Dughan *et al.*, 2013).

In wastewater, arsenic exists mainly in two inorganic forms: arsenite (As(III)) and arsenate (As(V)). As(III) is not only more toxic than As(V), but is also more difficult to remove from the wastewater (Styblo *et al.*, 2000; Korte and Fernando, 1991). In order to effectively remove arsenic from wastewater, it is necessary to oxidize As(III) to As(V) before the precipitation step (Khuntia, Majumder, and Ghosh, 2014; Leupin and Hug, 2005; Guan *et al.*, 2009). Although a few per cent of As(III) can be oxidized to As(V) within several days in the presence of air (Bissen and Frimmel, 2003), the oxidation rate is too slow for practical purposes. In order to increase the rate an advanced oxidation process such as the Fenton reaction can be used to remove hazardous substances from the wastewater. The Fenton reaction generates highly reactive hydroxyl radicals by the decomposition of hydrogen peroxide using ferrous ions (Pawar and Gawande, 2015). It has been shown that hydrogen peroxide can oxidize all As(III) to As(V) in 15 minutes (Arienzo, Chiarenzelli, and Scrudato, 2001). In the presence of Fe(II), the addition of hydrogen peroxide will produce free hydroxyl groups ($\cdot OH^-$), as shown in Equations [1]–[3], which will accelerate the oxidation of As(III) (Molnár *et al.*, 1994; Hug and Leupin, 2003):

Removal of arsenic and metal ions from acidic effluents *via* the Fenton reaction method

$$H_2O_2 + Fe^{2+} \rightarrow Fe^{3+} + OH^- + \cdot OH \qquad [1]$$

$$Fe^{2+} + \cdot OH \rightarrow Fe^{3+} + OH^- \qquad [2]$$

$$As^{3+} + \cdot OH \rightarrow As^{5+} + OH^- \qquad [3]$$

Therefore, the oxidation of As(III) to As(V) by hydrogen peroxide is an ideal way to remove arsenic from water. Our previous work (Wang *et al.*, 2018, 2019) has also confirmed that the optimim pH for removal of arsenic the pH range of 5–7, and the precipitates form as micrometre-sized particles with good stability.

In addition to arsenic, metallurgical wastewater may contain magnesium, copper, zinc, and other metal ions. These -ions not only have important economic value but also cause environmental pollution. During the arsenic co-precipitation process, both the arsenic and other metal ions will be adsorbed on the surface of ferrihydrite (Rout, Mohapatra, and Anand, 2012; Neupane, Donahoe, and Arai, 2014). Therefore, it is necessary to investigate the co-precipitation behaviour of arsenic and metal ions in the Fenton reaction process. In this study, hydrogen peroxide was used to oxidize Fe(II) and As(III) and remove the arsenic from an acidic effluent. The co-precipitation behaviour of several valuable metals and the stability of the precipitates were investigated.

Materials and experimental

Arsenic-bearing effluent synthesis

The arsenic-bearing effluent used in this work was collected by leaching arsenic from pyrite cinder using sulfuric acid at 90°C under atmospheric pressure. The leachate contained not only arsenic and iron, but also other metal ions including copper, zinc, magnesium, and aluminum. NaOH solution (20 wt.%) was added to the collected solution to adjust the pH to about 0.8. Then, the ferric concentration was measured using inductively coupled plasma-optical emission spectrometry (ICP-OES, Optima 8000). Iron powder was added to the solution in the molar ratio Fe (metal) to ferric ion of 1.5 to reduce Fe(III) to Fe(II) and the solution was stirred for about 6 hours at 50°C. The leaching solution was filtered using a vacuum filter to remove excess iron powder and other precipitates. The concentrations of arsenic and main metallic ions in the arsenic-bearing effluent are shown in Table I.

Oxidation-precipitation test by Fenton reaction

A volume of 100 mL of treated arsenic-bearing solution was put in a conical bottle, which was placed in a water bath pot. The solution was magnetically stirred at the desired temperature. The pH value was adjusted to the desired value using a 20% NaOH solution. Then, 30 wt.% hydrogen peroxide was dripped into the conical bottle according to the H_2O_2/As molar ratio. Meanwhile, 20% NaOH solution was added to the conical bottle to keep pH stable at a fluctuation range of 0.2. After stirring for different times, the pulp was separated quickly into solid and liquid using a vacuum pump so as to avoid the interference from the oxygen in the air. The precipitates were dried in a heating and drying oven (DHG-9240A)

at 1000C. Then, the precipitates were ground for the leaching toxicity test. The experiment procedure is shown in Figure 1.

The phase compositions of the precipitates were characterized by X-ray diffraction (XRD, X'Pert PRO MPD). The morphologies of the precipitates were determined by scanning electron microscopy with energy-dispersive spectroscopy (SEM-EDS, JSM-7001F). A laser particle size analyser (LS13-320) was used to determine the particle size distribution of the precipitates. The structures of the precipitates were investigated using Fourier transform infrared spectrometry (FTIR, Excalibur 3100). The metal ion concentrations in the filtrate were determined by ICP-OES.

Toxicity characteristic leaching

The test used for the toxicity characteristic leaching was China method HJ557-2010 (solid waste extraction procedure for leaching toxicity–horizontal vibration method). The acetate buffering solution of pH = 5±0.05 was used to leach the arsenic in the precipitates. One gram of precipitates and 10 millilitre acetate buffering solution were put into a 50 ml centrifuge tube which was fixed in a constant temperature oscillator with a vibrating frequency at 110 times/min. The solution was vibrated for 8 hours at room temperature and then allowed to stand for 16 hours. The mixture was passed through a quantitative filter paper to separate the solid and liquid, and the filtrate was analysed by ICP-OES.

Results and discussion

Effect of pH on coprecipitation

The pH value not only affects the crystallinity of ferric arsenate, but also has an important effect on the removal rate of arsenic. Generally, a lower pH (<1.2) is beneficial to the formation of crystalline ferric arsenate, but the removal rate of arsenic is slow at lower pH conditions (Min *et al.*, 2015). Increasing the pH value is beneficial to the removal of arsenic under acidic conditions. Our previous work (Wang *et al.*, 2018, 2019) has also confirmed that it is beneficial to remove arsenic in the pH range of 5–7, and the size of the precipitated particles can grow to 100 μm when Fe(II) is oxidized with hydrogen peroxide to co-precipitate arsenic. This work examined the effect of pH value on the co-precipitation behaviour of the metal ions and arsenic at a molar ratio of H_2O_2: As = 2, the setting pH fluctuation range of ±0.05, and one hour reaction time at ambient temperature (25°C). The results are shown in Figure 2.
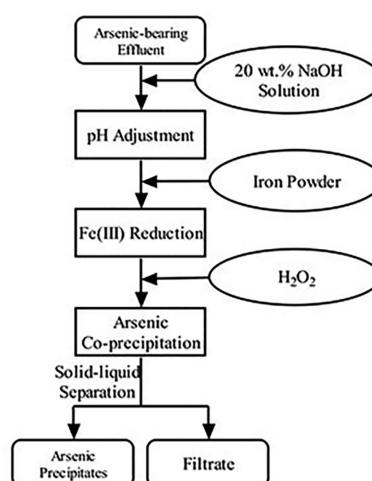

Figure 1—Flow chart of arsenic-bearing effluent pretreatment and co-precipitation

Table I

Concentrations of main impurity elements in the acidic leaching solution (mg/L)

Fe	As	Cu	Zn	Mg	Al
11 470	1038.1	20.6	19.2	386	365

Removal of arsenic and metal ions from acidic effluents *via* the Fenton reaction method
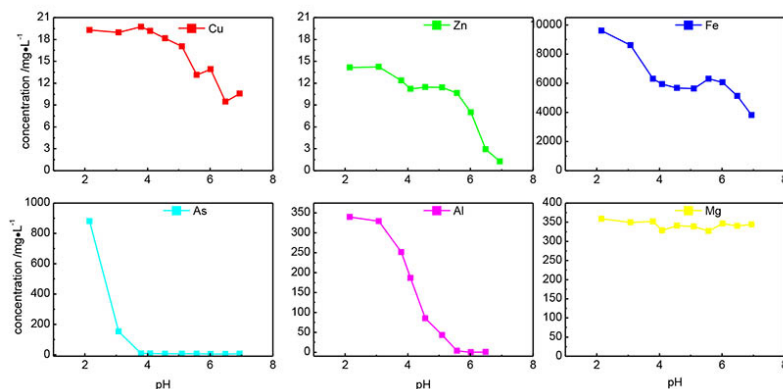

Figure 2—Effect of pH value on the removal of different elements in the solution

The results indicate that the concentrations of copper and zinc decrease slightly, which is primarily due to the fact that the initial contents of copper and zinc in the leaching solution are low. The magnesium concentration hardly decreases at all as the pH increases from 2.1 to 6.9, even though the initial magnesium concentration is up to 386 mg/L. The slight decrease in magnesium concentration may be explained by the adsorption of precipitates. The initial concentration of aluminum was 365 mg/L, and the results show that the aluminum gradually decreases with increasing pH value. The aluminum concentration decreased to 42.9 mg/L at a pH of 5.1. At pH values greater than 6, almost no aluminum remains in solution and its extraction is over 99%. The arsenic concentration decreased markedly with increasing pH. At a pH of 3.8 the arsenic concentration was only 8.4 mg/L; the decrease is not obvious when the pH increases from 3.8 to 6.5, and there is a minimum value of 3.1 mg/L at pH 6.5.

Iron in the initial solution is mainly in the form of Fe(II), some of which will be oxidized to Fe(III) after adding the hydrogen peroxide. When the pH increases from 2.1 to 3.9, the Fe concentration decreases from 9592 mg/L to 5903 mg/L. Fe(III) is precipitated in the pH range 2.1 to 3.9, and the residual iron in the solution is mainly in the form of Fe(II). The Fe concentration in the solution is virtually unchanged in the pH range 3.9–6.0, because Fe(II) precipitates with difficulty in this pH range. When the pH rises above 6.0, the Fe concentration once again decreases markedly, and a green precipitates can be observed due to the hydrolysis of Fe(II):

$$As^{3+} + \cdot OH \rightarrow As^{5+} + OH^- \qquad [4]$$

It will be seen that most of the Fe(III), As, Al, Zn, and Cu can be removed at pH 6.9. However, there is less impact on Mg due to the higher solubility product constants of $Mg(OH)_2$.

SEM results for the precipitates obtained under different pH conditions are presented in Figure 3. The results show that the surface of precipitates is smooth and neat at pH 2, and that the particle size is relatively uniform. More fine particles will appear as the pH increases (Fujita *et al.*, 2009). The results prove that the lower pH condition is beneficial to the growth of particles, which increases the stability of the precipitates (Min *et al.*, 2015; Fujita *et al.*, 2009). However, the lower pH is unfavourable for removing arsenic; a higher pH is necessary to obtain a high arsenic removal rate. In order to recycle the iron after co-precipitation, the pH should be controlled under 6.9 to reduce the precipitation of Fe(II). Therefore, a pH of 5.0–5.1 is chosen for the following discussion.

Effect of H₂O₂/As molar ratio on co-precipitation

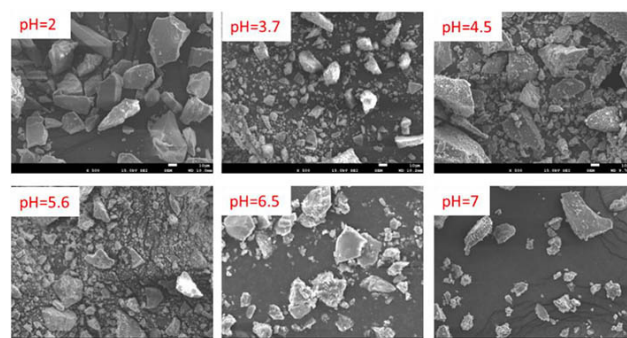Hydrogen peroxide (H_2O_2) is a strong oxidizing agent, especially in

Figure 3—SEM micrographs of the precipitates obtained under different pH conditions

the presence of Fe(II). The dosage of hydrogen peroxide will directly determine the molar ratio of Fe(III)/As for co-precipitation. The effect of H_2O_2/As molar ratio (HA) on co-precipitation was tested by controlling pH in the range of 5–5.1, with a water bath temperature of 25°C, and one hour reaction time.

More Fe(II) will be oxidized to Fe(III) with increasing hydrogen peroxide dosage, therefore, more arsenic can be co-precipitated as shown in Figure 4. For example, when the molar ratio of H_2O_2/As is 0.5, the concentrations of iron and arsenic in the solution are 9070 mg/L and 27.9 mg/L, respectively, decreasing to 5635 mg/L and 4.8 mg/L at H_2O_2/As = 2.0. The iron concentration continues to decrease as the H_2O_2/As increases to 3.0, but the arsenic concentration remains relatively stable.

The concentrations of Cu, Zn, and Mg do not change markedly with increasing H_2O_2. However, the aluminum concentration decreases. At a H_2O_2/As molar ratio of 0.5, the aluminum concentration is 68.1 mg/L, decreasing to 29.4 mg/L as H_2O_2/As increases to 3.0. This is because the aluminum can also be used to precipitate arsenic, and it is beneficial to the removal and stability of arsenic (Doerfelt *et al.*, 2016; Jia *et al.*, 2012). When more H_2O_2 is added to effluent, more As(III) is oxidized to As(V), which will co-precipitate with with Al(III) as well as with Fe(III). Therefore, the aluminum concentration decreases as the amount of H_2O_2 increases.

As the SEM micrographs in Figure 5 show, the particle size increases with the H_2O_2/As molar ratio. At a H_2O_2/As molar ratio of 0.5 most of the precipitate particles are smaller than 10 μm. The particle size increases as the H_2O_2/As molar ratio uncreases to 1.5, with many particles larger than 10 μm. At a H_2O_2/As molar ratio of 3.0, the particle size increases further, and some particles are even larger than 100 μm. A H_2O_2/As molar ratio of 2.0 was selected for the following discussion in order to reduce the dosage of hydrogen peroxide.
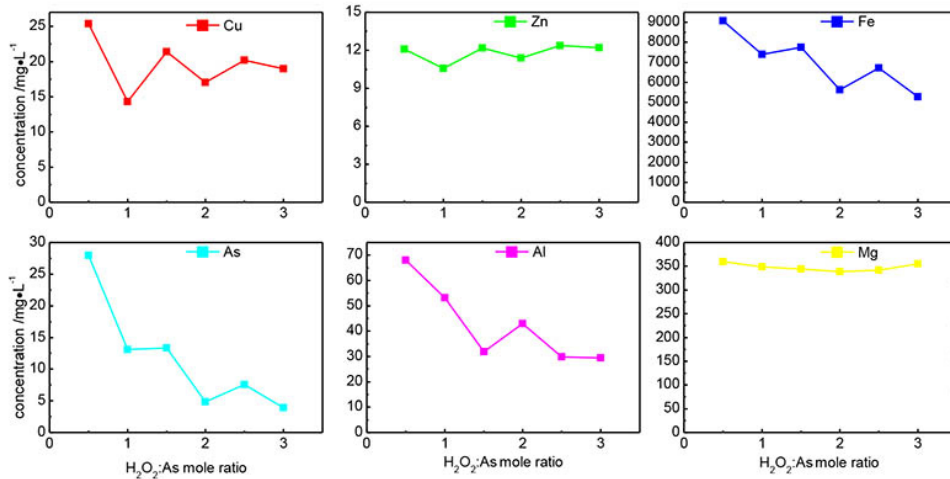
Figure 4—Effect of H₂O₂/As molar ratio on the precipitation of different elements
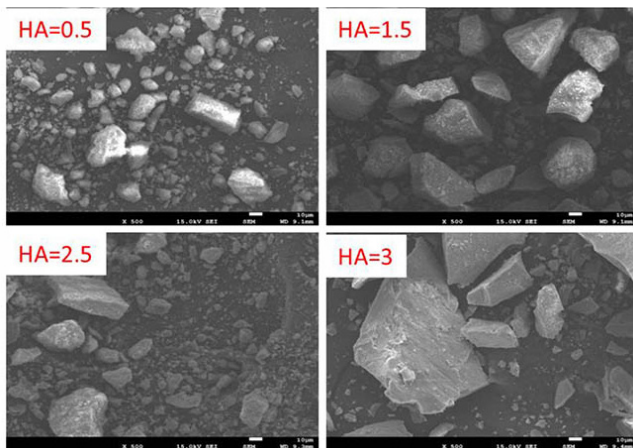

Figure 5—SEM micrographs of the precipitates obtained at different H₂O₂/As molar ratios

Effect of temperature on co-precipitation

Figure 6 shows the effect of increasing temperature under the conditions H₂O₂/As = 2.0, pH 5.0–5.2, and one hour reaction time. Temperature has little influence on the concentrations of Cu, Zn, and Mg, while the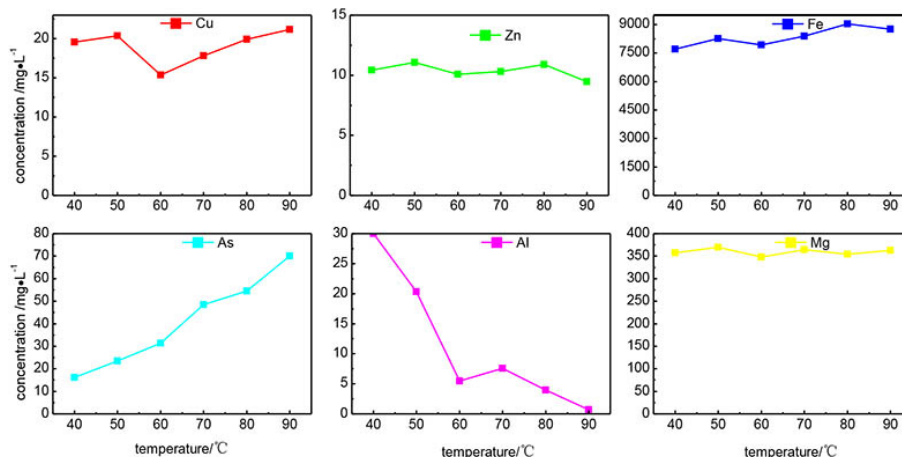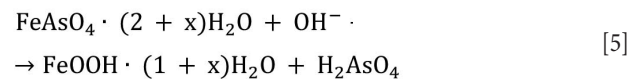 concentrations of iron and arsenic in solution increase with increasing temperature, from 7711 mg/L and 16.2 mg/L respectively at 40°C to 7940 mg/L and 31.4 mg/L at 60°C, and to 8760 mg/L and 70 mg/L at 90°C. The marked change in arsenic concentration may be closely related to the amorphous state of ferric arsenate under these conditions. The following decomposition reaction occurs (Berre, Gauvin, and Demopoulos, 2007):

$$FeAsO_4 \cdot (2 + x)H_2O + OH^- \cdot$$
$$\rightarrow FeOOH \cdot (1 + x)H_2O + H_2AsO_4 \quad [5]$$

As the temperature increases, the decomposition rate of ferric arsenate accelerates and more iron and arsenic return to the solution.

The aluminum concentration decreases with increasing temperature from 30 mg/L at 40°C to 5.5 mg/L at 60°C and 0.7 mg/L at 90°C. This is because increasing temperature favours the precipitation of Al (OH)₃ (Equation [6]) (Wei *et al.*, 2014).

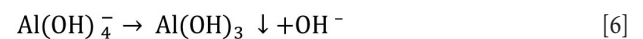$$Al(OH)_4^- \rightarrow Al(OH)_3 \downarrow + OH^- \quad [6]$$

Figure 7 shows the SEM micrographs of the precipitates obtained at different temperatures. It can be seen that the particle size is larger at temperatures less than 60°C. At temperatures greater than 70C, the particle surfaces are more porous, which is

Figure 6—Effect of temperature on the precipitation of different elements from solution
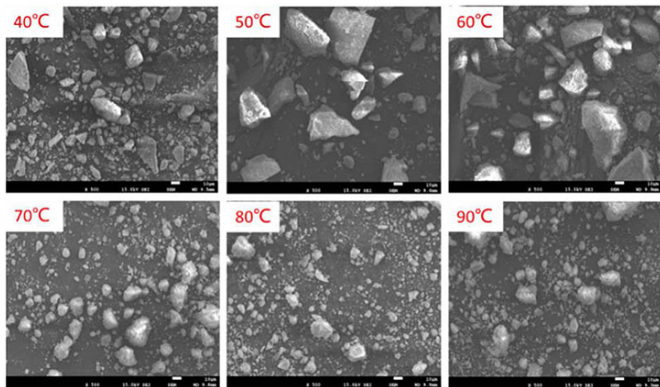
Figure 7—SEM micrographs of the precipitates obtained at different temperatures

detrimental to the stability of the sludge. These results indicate that lower temperatures are more favourable for precipitation. Therefore, ambient temperature was chosen as the experiment condition to investigate the effect of reaction time.

Effect of reaction time on co-precipitation

In order to investigate the effect of reaction time on the co-precipitation, a series of experiments was conducted under the following conditions: $H_2O_2/As = 2.0$, reaction temperature 25°C, and pH value between 5.1 and 5.3. The results in Figure 8 show that the concentrations of Fe, As, Zn, and Mg change little with extended reaction time, which indicates that the oxidation rate of Fe(II) by hydrogen peroxide is very fast, and the reaction is completed in a very short time to form amorphous ferric arsenate (Arienzo, Chiarenzelli, and Scrudato, 2001).

However, the concentrations of Cu and Al increased with reaction time, from 8.8 mg/L and 1.77 mg/L respectively at 10 minutes to 12.7 mg/L and 5.4 mg/L at 30 minutes, 19.2 mg/L and 35.4 mg/L at 90 minutes, and reaching 22.4 mg/L and 45.9 mg/L at 150 minutes. These results indicate that Cu and Al may be adsorbed on the surface of amorphous ferric arsenate, and are re-released into the solution with increasing time.

The SEM micrographs in Figure 9 show that the particle size increases with time. At the beginning, the particles are small with rough surfaces. The particle size increases and the surface becomes smooth as reaction time increases. The results indicate that an extended reaction time improves the precipitation.

In conclusion, higher removal rates of As, Cu, Zn, and Al can be achieved during arsenic co-precipitated by oxidation of Fe^{2+} with hydrogen peroxide at pH 5-6, $H_2O_2/As = 2.0$, ambient temperature, and atmospheric pressure. However, Mg is difficult to remove under these conditions due to the higher solubility product. The SEM micrographs show that the precipitates exist in the form of micrometre-sized particles, and the reaction conditions have an important influence on the surface morphology of the particles.

Characteristic of the precipitates

The precipitates obtained using the conditions of pH 5-6, $H_2O_2/As = 2$, reaction time 40 minutes, at room temperature and atmospheric pressure were subjected to XRD and FTIR analysis.

The XRD result (Figure 10) show that there are no obvious sharp peaks in the spectrum. There is just one broad band between $2\theta = 20–40°$, which indicates that the precipitates are amorphous. According to Berre, Gauvin, and Demopoulos (2007) this result is consistent with poorly crystalline ferric arsenate.

Figure 11 shows the FTIR spectrum of the co-precipitate in the range of 400–4000 cm⁻¹. The band at 840 cm⁻¹ is attributed to As–O stretching vibration of the As-O-Fe coordination (Müller *et al.*, 2010). The band at 480 cm⁻¹ is assigned to O-As-O bending vibration (Zhao, 1995). The bands located at 1627 cm⁻¹ and
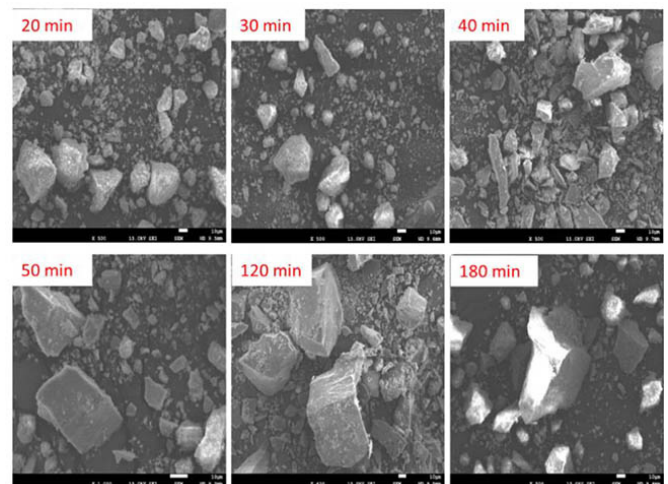

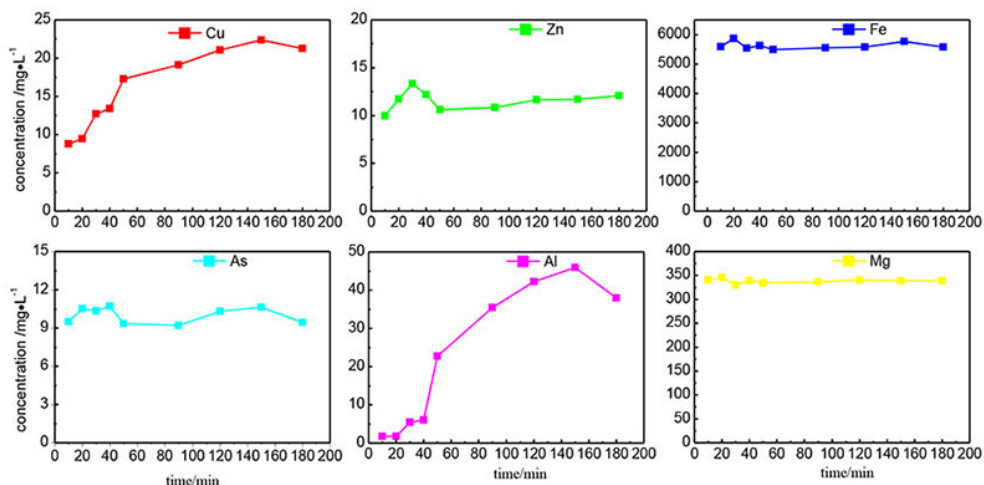**Figure 9—SEM micrographs of the precipitates obtained at different reaction times**

Figure 8—Effect of reaction time on the removal of different elements from solution
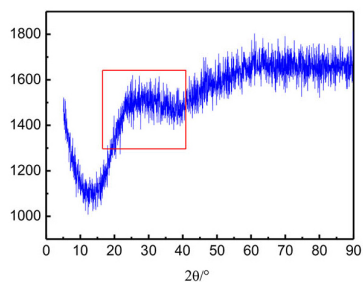
Figure 10—XRD spectrum of the co-precipitate
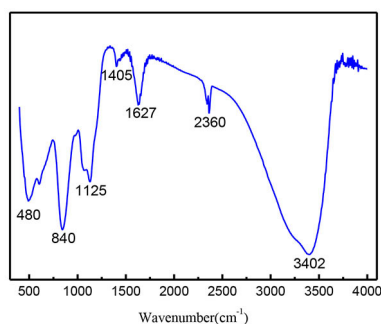
Figure 11—FTIR spectrum of the co-precipitate

Figure 12—SEM micrographs of the co-precipitates

Figure 13—Particle sizes distribution of the co-precipitates

Table II

Results of toxicity characteristic leaching test of the coprecipitates (mg/L)

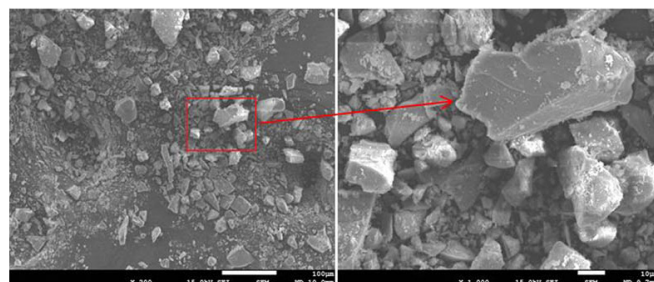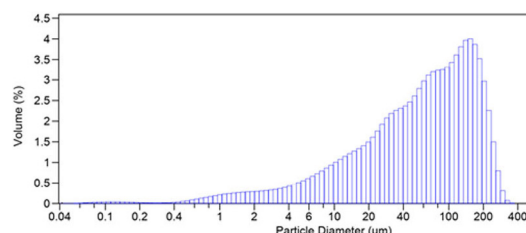| Fe	As	Cu	Zn	Mg	Al
–	3.56	–	–	–	81.4

3402 cm^{-1} exhibit strong O–H stretching and bending vibrations, respectively (Myneni *et al.*, 1998). The band at 1127 cm^{-1} may be the absorption peak of γ-FeOOH (Zhao, 1995). Therefore, it can be inferred that the co-precipitates mainly exists as ferric arsenate with amorphous rather than scorodite $FeAsO_4·2H_2O$.

The SEM micrographs in Figure 12 show the granular form of the precipitates, with particle sizes up to several tens of micrometred or even larger than 100 μm. The larger size is conducive to filtration of the precipitates. The particle size analysis (Figure 13) exhibits a fairly wide range, with an average size of 81.6 μm. The large-grained structure is beneficial to the stabilization of the co-precipitates. The local amplification result in Figure 12 shows that the particles do not comprise accumulations of fine particles, but are relatively dense and uniform. This structure is also beneficial to the stability of co-precipitates.

The results of the toxicity characteristic leaching test are shown in Table II. Fe, Cu, Zn, and Mg were not detected in the leachate. Iron in the precipitates is mainly in the trivalent form, and is only sparingly soluble in the acetic acid buffer at pH 5. The Cu, Zn, and Mg contents are very low in the co-precipitates, thus it is difficult to measure their contents in acetic acid leachate. The arsenic concentration is 3.6 mg/L, which meets the requirement of China national standards of < 5 mg/L (GB5085/3-2007). The concentration of Al is 81.4 mg/L, showing that the co-precipitation does not remove aluminum effectively. According to Doerfelt *et al.* (2016), the aluminum ion has a stabilizing effect on the precipitates, which is inconsistent with the findings of this study. This discrepancy may be a consequence of the amorphous nature of ferric arsenate, which has a strong adsorption capacity (Müller *et al.*, 2010). A large number of aluminum ions may be adsorbed on the surface of the co-precipitates, which will be re-dissolved into the toxicity characteristic test leachate. In addition, aluminum hydroxide is amphoteric, which may induce basic ionization in water (Equation [7]), and cause the solid $Al(OH)_3$ to break down again.

$$Al(OH)_3 \rightarrow Al^{3+} + 3OH^-$$ [7]

Therefore, the leaching concentration of Al is very high in the acetic acid buffer.

Conclusions

Acidic effluent containing arsenic and metal elements was treated by the Fenton reaction under atmospheric pressure. Most of the copper, zinc, and aluminum were removed under the conditions of pH 5–6, $H_2O_2/As = 2$ at ambient temperature. However, the removal of magnesium was negligible.

Increasing the pH and H_2O_2 dosage increased the removal of arsenic. However, increasing the temperature will decrease arsenic removal. In addition, a lower pH, lower temperature, and increased H_2O_2 dosage are beneficial to the growth of large particles.

The co-precipitates were mainly composed of amorphous ferric arsenate with an average particle size of 81.6 μm. The arsenic in the residue was stable, and its concentration in the leachate from the toxicity characteristic leaching test was only 3.6 mg/L. However, the aluminum in the co-precipitates is easily re-dissolved.

Acknowledgements

Data availability

All relevant data is included in the paper.

References

Ahmad, A., Rutten, S., Eikelboom, M., Waal, L., Bruning, H., Bhattacharya, P., and Wal, A. 2020. Impact of phosphate, silicate and natural organic matter on the size of Fe(III) precipitates and arsenate co-precipitation efficiency in calcium containing water. *Separation and Purification Technology*, vol. 235. pp. 116–117.

Ahoranta, S.H., Kokko, M.E., Papirio, S., Özkaya, B., and Puhakk J.A. 2016. Arsenic removal from acidic solutions with biogenic ferric precipitates. *Journal of Hazardous Materials*, vol. 306. pp. 124–132.

Removal of arsenic and metal ions from acidic effluents *via* the Fenton reaction method

Arienzo, M., Chiarenzelli, J., and Scrudato, R. 2001. Remediation of metal-contaminated aqueous systems by electrochemical peroxidation: an experimental investigation. *Journal of Hazardous Materials*, vol. B87, no. 1–3. pp. 187–198.

Berre, J.F.L., Gauvin, R., and Demopoulos G.P. 2007. Characterization of poorly-crystalline ferric arsenate precipitated from equimolar Fe(III)–As(V) solutions in the pH range 2 to 8. *Metallurgical and Materials Transactions*, vol. 38B. pp. 751–762.

Bissen, M. and Frimmel, F.H. 2003. Arsenic—a review. Part II: Oxidation of arsenic and its removal in water treatment. *Acta Hydrochimica et Hydrobiologica*, vol. 31, no. 2. pp. 97–107.

Chen, N., Jiang, D.T., Cutler, J., Kotzer, T., Jia, Y., Demopoulos, G.P., and Rowson, J.W. 2009 Structural characterization of poorly-crystalline scorodite, iron(III)-arsenate coprecipitates and uranium mill neutralized raffinate solids using X-ray absorption fine structure spectroscopy. *Geochimica et Cosmochimica Acta*, vol. 73, no. 11. pp. 3260–3276.

Davis, M.A., Signes-Pastor, A.J., Argos, M., Slaughter, F., Pendergrast, C., Punshon, T., Gossai, A., Ahsan, H., and Karagas, M.R. 2017. Assessment of human dietary exposure to arsenic through rice. *Science of the Total Environment*, vol. 586. pp. 1237–1244.

Doerfelt, C., Feldmann, T., Roy, R., and Demopoulos, G.P. 2016. Stability of arsenate-bearing Fe(III)/Al(III) co-precipitates in the presence of sulfide as reducing agent under anoxic conditions. *Chemosphere*, vol. 151. pp. 318–323.

Essilfie-Dughan, J., Hendry, M.J., Warner, J., and Kotzer, T. 2013. Arsenic and iron speciation in uranium mine tailings using X-ray absorption spectroscopy. *Applied Geochemistry*, vol. 28. pp. 11–18.

Fujita, T., Taguchi, R., Abumiya, M., Matsumoto, M., Shibata, E., and Nakamura T. 2009. Effect of pH on atmospheric scorodite synthesis by oxidation of ferrous ions: Physical properties and stability of the scorodite. *Hydrometallurgy*, vol. 96. pp. 189–198.

Guan, X., Dong, H., Ma, J., and Jiang, L. 2009. Removal of arsenic from water: Effects of competing anions on As(III) removal in $KMnO_4$–Fe(II) process. *Water Research*, vol. 43, no. 15. pp. 3891–3899.

Hering, J.G., Chen, P.Y., Wilkie, J.A., Elimelech, M., and Liang, S. 1996. Arsenic removal by ferric chloride. *JournalAWWA*, vol. 88, no. 4. pp. 155–167.

Hug, S.J. and Leupin, O. 2003. Iron-catalyzed oxidation of arsenic(III) by oxygen and by hydrogen peroxide: pH-dependent formation of oxidants in the Fenton reaction. *Environmental Science and Technology*, vol. 37, no. 12. pp. 2734–2742.

Jain, A., Raven, K., and Loeppert, R.H. 1999. Arsenite and arsenate adsorption on ferrihydrite: Surface charge reduction and net OH^- release stoichiometry. *Environmental Science and Technology,* vol. 33, no. 8. pp. 1179–1184.

Jia, Y., Xu, L., Wang, X. and Demopoulos, G.P. 2007 Infrared spectroscopic and X-ray diffraction characterization of the nature of adsorbed arsenate on ferrihydrite. *Geochimica et Cosmochimica Acta,* vol. 71. pp. 1643–1654.

Jia, Y., Zhang, D., Pan, R., Xu, L., and Demopoulos, G.P. 2012 A novel two-step coprecipitation process using Fe(III) and Al(III) for the removal and immobilization of arsenate from acidic aqueous solution. *Water Research*, vol. 46. pp. 500–508.

Khuntia, S., Majumder, S.K., and Ghosh, P. 2014. Oxidation of As(III) to As(V) using ozone microbubbles. *Chemosphere*, vol. 97. pp. 120–124.

Korte, N.E. and Fernando, Q. 1991. A review of arsenic(III) in groundwater. *Critical Reviews in Environmental Control*, vol. 21. pp. 1–39.

Leupin, O.X. and Hug, S.J. 2005. Oxidation and removal of arsenic(III) from aerated groundwater by filtration through sand and zero-valent iron. *Water Research*, vol. 39. pp. 1729–1740.

Mandal, B.K. and Suzuki, K.T. 2002. Arsenic round the world: A review. *Talanta,* vol. 58. pp. 201–235.

Mihajlovic I., Strbac N., Nikolic D., and Zivkovic Z. 2011. Potential metallurgical treatment of copper concentrates with high arsenic contents. *Journal of the Southern African Institute of Mining and Metallurgy*, vol. 111. pp. 409–416.

Min, X., Liao, Y., Chai, L., Yang, Z., Xiong, S., Liu, L., and Li, Q. 2015. Removal and stabilization of arsenic from anode slime by forming crystal scorodite. *Transactions of Nonferrous Metals Society of China*, vol. 25. pp. 1298–1306.

Molnár, L.U., Virčíková, E., and Lech, P. 1994. Experimental study of As (III) oxidation by hydrogen peroxide. *Hydrometallurgy*, vol. 35, no. 1. pp. 1–9.

Müller, K., Ciminelli, V.S., Dantas, M.S., and Willscher, S. 2010. A comparative study of As (III) and As (V) in aqueous solutions and adsorbed on iron oxy-hydroxides by spectroscopy. *Water Research*, vol. 44. pp. 5660–5672.

Myneni, S.C.B., Traina, S.J., Waychunas, G.A., and Logan, T.J. 1998. Experimental and theoretical vibrational spectroscopic evaluation of arsenate coordination in aqueous solutions, solids, and at mineral-water interfaces. *Geochimica et Cosmochimica Acta*, vol. 62, no. 19/20. pp. 3285–3300.

Neupane, G., Donahoe, R.J., and Arai, Y. 2014. Kinetics of competitive adsorption/desorption of arsenate and phosphate at the ferrihydrite–water interface. *Chemical Geology*, vol. 368. pp. 31–38.

Otgon, N., Zhang, G., Zhang, K., and Yang, C. 2019. Removal and fixation of arsenic by forming a complex precipitate containing scorodite and ferrihydrite. *Hydrometallurgy*, vol. 186. pp. 58–65.

Qiao, J, Jiang, Z., Sun, B., Sun, Y., Wang, Q., and Guan, X. 2012. Arsenate and arsenite removal by $FeCl_3$: Effects of pH, As/Fe ratio, initial As concentration and co-existing solutes. *Separation and Purification Technology*, vol. 92. pp. 106–114.

Pawar, V. and Gawande, S. 2015. An overview of the Fenton Process for industrial wastewater. *IOSR Journal of Mechanical and Civil Engineering*, vol. 2. pp. 127–136.

Rout, K., Mohapatra, M., and Anand, S. 2012. 2-Line ferrihydrite: synthesis, characterization and its adsorption behavior for removal of Pb(II), Cd(II), Cu(II) and Zn(II) from aqueous solutions. *Dalton Transactions*, vol. 41. pp. 3302–3312.

Singh, R., Singh, S., Parihar, P., Singh, V.P., and Prasad, S.M. 2015. Arsenic contamination, consequences and remediation techniques: A review. *Ecotoxicology and Environmental Safety*, vol. 112. pp. 247–270.

Styblo, M., Razo, L.M., Vega, L., Germolec, D.R., LeCluyse, E.L., Hamilton, G.A., Reed, W., Wang, C., Cullen, W.R., and Thomas, D.J. 2000. Comparative toxicity of trivalent and pentavalent inorganic and methylated arsenicals in rat and human cells. *Archives of Toxicology*, vol. 74. pp. 289–299.

Tang, Y., Wang, J., and Gao, N. 2010. Characteristics and model studies for fluoride and arsenic adsorption on goethite. *Journal of Environmental Sciences*, vol. 22, no. 11. pp. 1689–1694.

Türk, T., Alp, İ., Sezer, R., and Arslan, C. 2020. Removal of arsenic from water using copper slag. *Journal of the Southern African Institute of Mining and Metallurgy*, vol. 120. pp. 313–318.

Wang, Y., Lv, C., Xiao, L., Fu, G., Liu, Y., Ye, S., and Chen, Y. 2019. Arsenic removal from alkaline leaching solution using Fe (III) precipitation. *Environmental Technology*, vol. 40, no. 13. pp. 1714–1720.

Wang, Y., Xiao, L., Liu, H., Qian, P., Ye, S., and Chen, Y. 2018 Acid leaching pretreatment on two-stage roasting pyrite cinder for gold extraction and co-precipitation of arsenic with iron. *Hydrometallurgy*, vol. 179. pp. 192–197.

Wei, G., Qu, J., Zheng, Y., Qi, T., Guo, Q., Han, B., and Zhao, H. 2014 Crystallization behaviors of bayerite from sodium chromate alkali solutions. *Transactions of Nonferrous Metals Society of China*, vol. 24. pp. 3356–3365.

Wickramasinghe, S.R., Han, B.B., Zimbron, Z., Shen, Z., and Karim, M.N. 2004. Arsenic removal by coagulation and filtration: Comparison of groundwaters from the United States and Bangladesh. *Desalination*, vol. 169, no. 3. pp. 231–244.

Zhu, Y., Zhang, X., Xie, Q., Wang, D., and Cheng, G. 2006. Solubility and stability of calcium arsenates at 25°C. *Water, Air, and Soil Pollution*, vol. 169, no. 1–4. pp. 221–238.

Zhao, Z. 1995. Mechanism of arsenic removal in oxidized Fe-As system. China *Environmental Science*, vol. 15., pp. 18–21 [in Chines ◆